# Improving Low-Temperature Catalysis in the Hyperthermostable *Pyrococcus furiosus* β-Glucosidase CelB by Directed Evolution†

Joyce H. G. Lebbink,‡ Thijs Kaper, Peter Bron, John van der Oost,* and Willem M. de Vos

*Laboratory of Microbiology, Wageningen University, Hesselink van Suchtelenweg 4, 6703 CT Wageningen, The Netherlands*

*Received June 28, 1999; Revised Manuscript Received December 31, 1999*

ABSTRACT: The β-glucosidase from the hyperthermophilic archaeon *Pyrococcus furiosus* (CelB) is the most thermostable and thermoactive family 1 glycosylhydrolase described to date. To obtain more insight in the molecular determinants of adaptations to high temperatures and study the possibility of optimizing low-temperature activity of a hyperthermostable enzyme, we generated a library of random CelB mutants in *Escherichia coli*. This library was screened for increased activity on *p*-nitrophenyl-β-D-glucopyranoside at room temperature. Multiple CelB variants were identified with up to 3-fold increased rates of hydrolysis of this aryl glucoside, and 10 of them were characterized in detail. Amino acid substitutions were identified in the active-site region, at subunit interfaces, at the enzyme surface, and buried in the interior of the monomers. Characterization of the mutants revealed that the increase in low-temperature activity was achieved in different ways, including altered substrate specificity and increased flexibility by an apparent overall destabilization of the enzyme. Kinetic characterization of the active-site mutants showed that in all cases the catalytic efficiency at 20 °C on *p*-nitrophenyl-β-D-glucose, as well as on the disaccharide cellobiose, was increased up to 2-fold. In most cases, this was achieved at the expense of β-galactosidase activity at 20 °C and total catalytic efficiency at 90 °C. Substrate specificity was found to be affected by many of the observed amino acid substitutions, of which only some are located in the vicinity of the active site. The largest effect on substrate specificity was observed with the CelB variant N415S that showed a 7.5-fold increase in the ratio of *p*-nitrophenyl-β-D-glucopyranoside/*p*-nitrophenyl-β-D-galactopyranoside hydrolysis. This asparagine at position 415 is predicted to interact with active-site residues that stabilize the hydroxyl group at the C4 position of the substrate, the conformation of which is equatorial in glucose-containing substrates and axial in galactose-containing substrates.

Carbohydrate polymers can be degraded by a wide variety of glycosylhydrolases that have been classified into more than 70 different families on the basis of amino acid sequence comparisons (http://afmb.cnrs-mrs.fr/~pedro/CAZY/db.html) (*1*, *2*). In recent years, considerable progress has been achieved in the determination and characterization of primary and three-dimensional structures from family 1 glycosylhydrolases. Of the family 1 enzymes isolated from mesophiles, the crystal structures have been solved of the 6-phospho-β-galactosidase (LacG) from *Lactococcus lactis* and the β-glucosidase from *Bacillus polymyxa* (*3*−*5*). Both of these enzymes have been cocrystallized with either the substrate or an inhibitor in the active site and therefore allow analysis of the interactions between the enzyme and its substrate. Biochemical characterization and primary structure determination have been reported for several family 1 glycosylhydrolases from hyperthermophilic organisms, that optimally grow at and around the normal boiling point of water. These include the β-glucosidase from *Thermotoga maritima* (*6*), the β-glycosidase LacS from *Sulfolobus solfataricus* (*7*, *8*) and the β-glucosidase CelB and β-mannosidase BmnA from *Pyrococcus furiosus* (*9*−*11*). The crystal structure of LacS as well as the structure of the β-glycosidase from *Thermosphaera aggregans* have recently been reported (*12*, *13*). A three-dimensional model for CelB, based on 3.3 Å X-ray diffraction data, is available (*39*, *40*). The comparison of these structures with the homologous structures from the mesophiles allows for studying of the molecular adaptations of family 1 enzymes to high temperatures.

We have focused on the most thermostable member of the family 1 glycosyl hydrolases, CelB from the archaeon *P. furiosus*. CelB was purified from *P. furiosus*, characterized, and found to be a tetrameric enzyme of 230 kDa with identical 58 kDa subunits (*10*). The enzyme is very well adapted to the high growth optimum of the organism (100 °C), with a half-life for thermal inactivation of 85 h at 100 °C and an optimum temperature for activity of 102−105 °C. CelB shows high activity on the aryl glucosides *p*-nitrophenyl β(1,4)-D-glucopyranoside (pNp-Glc) and *p*-nitrophenyl β(1,4)-D-galactose (pNp-Gal), as well as on β(1,4)-linked disaccharides cellobiose and lactose and on the β(1,3)-linked disaccharide laminaribiose (*10*, *14*). Low activity was

† This work has been partially supported by Contracts BIOT-CT93-0274 and BIO 4-CT96-0488 of the European Union.

* To whom correspondence should be addressed: Phone 31 317 483110; Fax 31 317 483829; email john.vanderoost@algemeen.micr.wau.nl.

‡ Present address: Karolinska Institutet, Novum, Center for Structural Biochemistry, S-14157 Huddinge, Sweden.

[1] Abbreviations: pNp, *p*-nitrophenol; pNp-Glc, *p*-nitrophenyl-β-D-glucopyranoside; pNp-Gal, *p*-nitrophenyl-β-D-galactopyranoside; X-Glc, 5-bromo-4-chloro-3-indolyl-β-D-glucopyranoside; X-Gal, 5-bromo-4-chloro-3-indolyl-β-D-galactopyranoside.

10.1021/bi991483q CCC: $19.00 
Published on Web 03/10/2000

detected on pNp-mannose and pNp-xylose. The *celB* gene was cloned, sequenced, and functionally overexpressed in *Escherichia coli* (*9*). By site-directed mutagenesis, Glu 372 was identified as the active-site nucleophile, being the equivalent of the nucleophile in mesophilic homologues according to a multiple sequence alignment (*9*). Moreover, a recent study indicated that the enzymes from *P. furiosus* and the mesophilic bacterium *Agrobacterium faecalis* share a common catalytic mechanism (*15*). The three-dimensional model for CelB shows that the conformation of the active site is identical to that of other family 1 enzymes (*39*, *40*).

An alternative approach to study structure−function relations in enzymes is that of directed evolution by combining random mutagenesis, in vitro recombination, and rapid screening procedures (*16*−*18*). Subsequent biochemical and structural analysis of selected mutant enzymes has been shown to contribute to understanding the molecular basis of the observed phenotypic changes and as such to our knowledge of enzyme catalysis and stability. Directed evolution approaches have hitherto been restricted to enzymes with moderate thermostability and have not yet been applied to enzymes from hyperthermophiles. CelB is extremely suitable to be used as a hyperthermostable model enzyme in the development of such a procedure, since it is efficiently produced in *E. coli*, is not posttranslationally modified, and is capable of hydrolyzing chromogenic substrates at both low and high temperatures. In this study we describe the construction of a random CelB library and the screening of this library for increased activity on pNp-glucose at room temperature. Multiple random mutants were selected and characterized, with the aim to gain insight into substrate recognition and catalysis at both low and high temperatures and into the relation of these features with thermoactivity and thermostability.

## MATERIALS AND METHODS

*Construction of a Random Mutant CelB Library*. Random mutations were introduced into the *celB* gene on pLUW511 (*40*) by PCR amplification with primers BG238 (5′-GCGCGCCATGGCAAAGTTCCCAAAAAACTTCATGTTTG; *Nco*I restriction site underlined) and BG309 (5′-GTTAGCAGCCGGATCCCTA; *Bam*HI restriction site underlined) and proofreading-deficient *Taq* DNA polymerase (Pharmacia, Uppsala, Sweden). DNA shuffling of the *celB* gene was performed essentially according to the protocol of Stemmer (*16*) with the optimization described by Lorimer and Pastan (*19*). The resulting shuffled DNA fragments were digested with *Nco*I and *Bam*HI, the restriction sites of which overlapped the *celB* start and stop codons, respectively. The fragments were subsequently cloned into expression vector pET9d as a translational fusion with phage $\phi$10 translation initiation and termination signals (*20*). The resulting plasmids were used to transform *E. coli* JM109(DE3) (*21*, *22*). Transformation mixtures were plated onto selective TY agar plates (1% tryptone, 0.5% yeast extract, and 0.5% NaCl, with 1.5% granulated agar and 30 $\mu$g/mL kanamycin) supplemented with 16 $\mu$g/mL of the chromogenic substrate 5-bromo-4-chloro-3-indolyl-$\beta$-D-glucopyranoside (X-Glc, Biosynth, Switzerland). Transformants harboring only pET9d or nonfunctional *celB* variants will remain white after overnight growth at 37 °C, while transformants harboring functional *celB* genes will develop a blue color due to hydrolysis of the X-Glc. Single blue colonies were transferred to microtiter plates containing 200 $\mu$L/well TY broth supplemented with 30 $\mu$g/mL kanamycin.

*Screening for Increased Activity on pNp-Glc at Room Temperature*. A replica of the random CelB library was prepared in microtiter plates and bacterial growth was quantified by determination of the optical density at 560 nm with a Thermomax microplate reader (Molecular Devices). Data were exported into a spreadsheet (Excel, Microsoft) and corrected for blank absorption. *E. coli* cells were lysed by a combination of freezing/thawing and addition of 10 $\mu$L of chloroform and 5 $\mu$L of 0.1% SDS. No negative effect of these additives on CelB activity was detected in control experiments. Viscosity was reduced by adding 10 $\mu$g/mL DNase I and 10 mM $MgCl_2$. CelB activity at 20 °C was assayed by transfer and mixing of 5 $\mu$L of lysed cells to a second set of microtiter plates containing 100 $\mu$L/well 150 mM sodium citrate (pH 4.8) and 1 mM pNp-Glc. After 30 min reactions were stopped by addition of 200 $\mu$L of 0.5 M $Na_2CO_3$. Free pNp formation was quantified at 405 nm with the Thermomax microplate reader. Potential high-performance mutants were selected on the basis of an increased ratio of $OD^{405nm}/OD^{560nm}$ relative to wild-type controls. These mutants were regrown and rescreened according to the same procedure. Plasmid DNA of confirmed high-performance mutants was subjected to a second round of mutation and selection.

*Characterization of High-Performance Mutants*. High-performance mutants were grown overnight in 10 mL of selective TY medium at 200 rpm. Cells were spun down, resuspended in 1 mL of a 20 mM sodium citrate buffer (pH 4.8), and lysed by sonication (Branson sonifier). Cell debris was spun down and cell-free extract was incubated for 10 min at 80 °C. Denatured *E. coli* proteins were precipitated by centrifugation. Protein concentration of the heat-stable cell-free extract was determined according to Bradford (*23*) using the Bio-Rad protein assay (Biorad, Veenendaal, The Netherlands). SDS−PAGE analysis revealed that CelB was at least 90% pure in heat-stable cell-free extract (not shown). CelB activity at 20 and 90 °C was determined relative to that of wild-type CelB in 0.5 of mL 150 mM sodium citrate (pH 4.8), containing 3 mM pNp-Glc or 40 mM pNp-Gal. The pNp-Glc concentration was chosen as 3 mM because at higher concentrations the occurring substrate inhibition will cause an underestimation of the enzyme activity. pNp-Gal could be used at 40 mM since there is no indication at all for substrate inhibition for the wild-type CelB and any of the characterized mutant enzymes. Reactions were stopped by addition of 1 mL of 0.5 M $Na_2CO_3$ and the free pNp concentration was quantified at 405 nm on a Hitachi U-1100 spectrophotometer. Temperature optima were determined in 150 mM sodium citrate buffer (pH 4.8) containing 3 mM pNp-Glc at desired temperatures up to 98 °C in a water bath. Thermostability was analyzed in an oil bath at 106 °C. Heat-stable cell-free extract was diluted to 50 $\mu$g/mL protein in a 20 mM sodium citrate buffer, pH 4.8. Samples (100 $\mu$L) were incubated in glass vials closed by screw caps with Teflon inlay and incubated at 106 °C. Residual CelB activity after 1 h of incubation was determined at 20 °C as described above and compared to the activity of a sample kept at room temperature.

*DNA Sequencing and Three-Dimensional Structure Analysis*. Plasmid DNA was isolated from 3 mL cultures by using the Qiaprep spin plasmid kit (Qiagen, Westburg, The Netherlands) according to the included protocol. Sequencing was performed with infrared-labeled oligos (MWG, Germany), complementary to pET9d sequences immediately flanking the cloning site on the plasmid, and the Thermo Sequenase kit (Amersham Life Science) on the Li-Cor 4000L automated sequencer. Amino acid substitutions were deduced from identified mutations in the DNA sequence of the *celB* gene, and their position and possible interactions in the three-dimensional structure of CelB were analyzed by using the 3D structures of BglA from *B. polymyxa* (*5*; PDB accession code 1bgg.pdb) and LacS from *S. solfataricus* (*12*; PDB accession code 1gow.pdb) and the three-dimensional model for CelB (*39*, *40*), with the use of the molecular visualization software Rasmol (Raswin Molecular Graphics version 2.6; Sayle, Glaxo Research and Development, U.K.) on a personal computer, and InsightII (V 97.0, Molecular Simulations Inc.) on a Silicon Graphics Indy workstation.

*Purification of CelB and Determination of Biochemical Parameters*. One liter of selective TY medium in 2 L baffled Erlenmeyer flasks was inoculated with *E. coli* harboring expression plasmids containing either wild-type or mutant *celB* genes and cultured overnight at 37 °C with vigorous shaking. Cell lysate was prepared and CelB was purified with heat precipitation and anion-exchange chromatography essentially as described (*9*) with an additional gel filtration in 20 mM Tris-HCl buffer (pH 8.0) on a 300 mL Superdex 75 column (Pharmacia, Sweden). Pure CelB fractions were pooled and dialyzed against 20 mM sodium citrate buffer (pH 4.8). Protein concentrations were determined at 280 nm with an extinction coefficient for one subunit of $\epsilon_m^{280nm} = 1.28 \times 10^5\ M^{-1}\ cm^{-1}$ according to Gill and von Hippel (*24*). Initial CelB activity of pure fractions was monitored continuously in a total volume of 1.0 mL of 150 mM sodium citrate buffer (pH 4.8, set at 20 °C) at 20 and 90 °C on a Hitachi U-2010 spectrophotometer equipped with an SPR-10 temperature controller (Hitachi, Tokyo, Japan).

The amount of wild-type and mutant CelB in the activity assays on pNp-Glc/Gal and cellobiose/lactose was in the range of 5−20 $\mu$g at 20 °C and 90−240 ng at 90 °C. Formation of hydrolyzed pNp was measured at 405 nm. Catalytic activities were calculated by using extinction coefficients for pNp in the assay buffer of $\epsilon_m^{405nm} = 0.178\ mM^{-1}\ cm^{-1}$ at 20 °C and $\epsilon_m^{405nm} = 0.561\ mM^{-1}\ cm^{-1}$ at 90 °C. Turnover rates ($k_{cat}$, in reciprocal seconds) were calculated from the subunit molecular weight of CelB $M_r = 54{,}580$ Da. A turnover rate of 0.967 $s^{-1}$ corresponds to a catalytic activity of 1 unit/mg, in which 1 unit is defined as the amount of $\beta$-glucosidase activity needed to catalyze the liberation of 1 $\mu$mol of *p*-nitrophenol/min at the given temperature. Kinetic parameters were determined by measuring initial velocity at varying substrate concentrations, ranging from 0 to 8 mM pNp-Glc (up to 40 mM for N415S at 90 °C) and 0.2−40 mM pNp-Gal. Hydrolysis of disaccharides was performed in 150 mM citrate buffer (pH 4.8) with 0−150 mM cellobiose or 0−300 mM lactose at 20 and 90 °C. Glucose formation was quantified by use of the Peridochrom glucose kit (Boehringer Mannheim, Germany) according to the included protocol. The signals of the reaction substrates cellobiose and lactose and the product galactose were found to be negligible. For each $K_m$ and $k_{cat}$ determination, at least 14 substrate/velocity data pairs were determined. Kinetic data were fitted according to functions describing Michaelis−Menten kinetics or, when necessary, according to a second-degree function describing substrate inhibition by using the nonlinear regression program Tablecurve (Tablecurve 2D for Windows, version 2.03, Jandel Scientific). In the second-degree inhibitor function, a $[S]^2$ term has been added to the denominator of the Michaelis−Menten equation.

The formation of reaction products after 30 min of incubation at 20 and 90 °C of 20 $\mu$g of wild-type CelB with 20 and 150 mM cellobiose was analyzed by HPLC using a Polyspher OAHY column (Merck, Darmstadt, Germany). Solutions (20 mM) of glucose, cellobiose, and a mixture of cellulodextrines were used as standards. Thermal inactivation of pure enzyme samples was studied by incubation of 50 $\mu$g/mL samples of wild-type and mutant CelB at 106 °C in 20 mM sodium citrate buffer (pH 4.8). Remaining activity as a function of time was assayed relative to a standard kept at room temperature. First-order plots of inactivation yielded half-life values for thermal inactivation.

## RESULTS AND DISCUSSION

*Construction of a Random Mutant CelB Library*. The hyperthermostable $\beta$-glucosidase CelB from *P. furiosus* is optimally active at 102−105 °C, and its activity at room temperature does not exceed 1% of its optimal activity. To study the possibility of increasing this low activity at room temperature and in order to gain more insight into the factors determining this temperature dependence of activity, we subjected the *celB* gene to random mutagenesis and low-temperature activity screening. Random mutations were introduced into the *celB* gene by use of error-prone PCR and in vitro recombination by DNA shuffling according to Stemmer (*16*). After the mutated *cel*B genes were cloned in *E. coli*, transformants harboring functional CelB enzymes were selected by their ability to hydrolyze the chromogenic substrate analogue X-Glc at low temperature. An ordered library consisting of 6160 random *E. coli* mutants was constructed. Complete DNA sequence analysis of nine randomly picked mutants revealed an average mutation frequency of 2.3 base pairs/*celB* gene, indicating that on average 1 or 2 amino acids will be changed in each CelB enzyme (data not shown).

*Screening for Increased Activity on pNp-Glc at Room Temperature*. The mutant CelB library was screened for increased activity on pNp-Glc at room temperature. This resulted in the identification of about 400 mutants with significantly higher activity than the wild-type controls. These mutants were transferred to new microtiter plates and rescreened. Heat-stable cell-free extracts of the 42 most active mutants were further analyzed for low-temperature $\beta$-glucosidase activity. Eventually, the nine most active mutants (harboring plasmids pLUW838−pLUW846) were selected, analyzed in detail, and found to contain heat-stable $\beta$-glucosidase activities that were up to 3-fold higher at room temperature than that of *E. coli* producing wild-type CelB (Table 1). Variation in enzyme production levels was ruled out as an explanation for this increased activity since protein analysis by SDS−PAGE showed that CelB expression levels were similar in all mutants (data not shown). Plasmid inserts

Table 1: Characterization of High-Performance CelB Mutants[a]

| plasmid pLUW | amino acid substitution(s) | class | % act. on pNp-Glc at 20 °C | % act. on pNp-Gal at 20 °C | % act. on pNp-Glc at 90 °C | % act. on pNp-Gal at 90 °C | temperature optimum (°C) | thermostability (% residual act. after 1 h at 106 °C) |
|---|---|---|---|---|---|---|---|---|
| pLUW511 | wild type | | 100 | 100 | 100 | 100 | ≥98 | 100 |
| pLUW839 | N415S | I | 259 | 64 | 35 | 35 | ≥98 | 100 |
| pLUW842 | M424V | I | 199 | 140 | 53 | 49 | 85 | 24 |
| pLUW843 | T371A | I | 148 | 139 | 101 | 91 | 85−90 | 14 |
| pLUW846 | A419T | I | 159 | 109 | 64 | 98 | 85 | 53 |
| pLUW844 | K285R | III | 155 | 103 | 55 | 81 | 85−90 | 58 |
| pLUW841 | V211A | I | 260 | 151 | 141 | 120 | 85−90 | <1 |
| | V163I | II | | | | | | |
| | F447S | II | | | | | | |
| pLUW847[b] | N415S | I | 308 | 27 | 24 | 63 | 85 | <1 |
| | V211A | I | | | | | | |
| | Y227H | II | | | | | | |
| | E26G | III | | | | | | |
| pLUW845 | I161V | II | 110 | 37 | 86 | 125 | 98 | 84 |
| | E119G | III | | | | | | |
| pLUW840 | K70R | II | 175 | 147 | 42 | <1 | 70−80 | <1 |
| | L45P | II | | | | | | |
| | F344L | III | | | | | | |
| pLUW838 | I67T | III | 110 | 97 | 70 | 70 | ≥98 | 100 |
| | D159N | III | | | | | | |
| | A341T | III | | | | | | |

[a] For each mutant the amino acid substitutions are listed, as well as their classification. Class I involves amino acid substitutions in the active-site region; Class II, at or very near to the subunit interfaces, and class III, at the surface of the protein or buried in the interior and not in one of the other categories. Specific activities on 3 mM pNp-Glc and 40 mM pNp-Gal at 20 and 90 °C were determined and are listed in percentages relative to wild-type CelB; absolute values of specific activities of wild-type CelB are 13.4 units/mg with pNp-Glc at 20 °C, 9.4 units/mg with pNp-Gal at 20 °C, 1655 units/mg with pNp-Glc at 90 °C, and 2482 units/mg with pNp-Gal at 90 °C (see also Tables 2 and 3). Temperature optima were determined up to 98 °C, and thermostability relative to the wild type was determined at 106 °C. [b] pLUW847 was selected from a second-generation library.

were sequenced and amino acid substitutions were deduced from the changes in the DNA sequence (Table 1).

*Amino Acid Substitutions in High-Performance Mutants*. The three-dimensional model of CelB (*39*, *40*), and the crystal structures of LacS (*12*) and BglA from *B. polymyxa* complexed with gluconate in the active site (*5*) were used to analyze the position and possible interactions of each of the amino acid substitutions found in the high-performance mutants. LacS is a close relative of CelB (53% amino acid identity), with an identical arrangement of subunits into a tetrameric conformation. BglA is distantly related, with only 17% amino acid identity but 100% conservation of the active-site residues (all residues depicted in Figure 3 are identical in both CelB and LacS as well as in BglA). Because of the low resolution of the present CelB model, we have been careful in evaluating interactions and mainly restricted this to the active-site region, where high structural homology between CelB, LacS, and BglA is found. In other regions we restricted the analysis to an evaluation of the position of the mutations and expected general effects.

The position of the identified amino acid substitutions is marked in the CelB sequence in a multiple amino acid sequence alignment, which furthermore highlights the active-site residues and residues involved in intersubunit contacts (Figure 1). Analysis of the position of the substitutions in the CelB model revealed a more or less uniform distribution over the enzyme (Figure 2). On the basis of the position of the substitutions in the enzyme structure, three classes of CelB mutants were distinguished (Table 1, Figure 2). The first class (class I) involves substitutions of residues in the immediate vicinity of the active site that often directly interact with active-site residues. The second class (class II) involves substitutions that are located at or near subunit interfaces. The remainder of the mutations were assigned to class III and involve substitutions at the protein surface or buried in the interior of the monomers. Five of the high-performance mutants contained single amino acid substitutions. While in these mutants the genotype−phenotype relation is straightforward, this is less clear in the remaining mutants containing multiple amino acid substitutions.

The majority of the amino acid substitutions in those mutants containing only a single substitution belong to class I (Figure 3). These mutations predominantly affect the C-terminal part of the enzyme. Plasmid pLUW839 encodes amino acid substitution N415S, which involves an asparagine residue that is hydrogen-bonded to active-site residues glutamine 17 and glutamate 417. These two residues directly interact with the hydroxyl group at the C4 position of the substrate. The serine side chain in the mutant is much shorter than the original asparagine. Therefore, interactions will be significantly weakened or destroyed and a cavity may be introduced. In homologous family 1 glycosylhydrolases this residue is conserved except for *L. lactis* LacG (and other 6-phospho-$\beta$-galactosidases), which contains a valine (or a leucine or glutamine) at this position (Figure 1) (*25*). Mutant N415S displays the highest increase in $\beta$-glucosidase activity and is as thermostable as the wild-type enzyme. DNA of pLUW839, coding for this mutant, was therefore used to start a second-generation evolution, resulting in a derivative (harboring pLUW847) with considerably higher activity on pNp-Glc than the N415S mutant CelB (Table 1).

Plasmid pLUW842 encodes the single amino acid substitution M424V, which involves a methionine that, like the asparagine at position 415, contacts active-site glutamate 417. The valine in the resulting mutant CelB introduces a shorter but more bulky side chain that may influence the conforma-

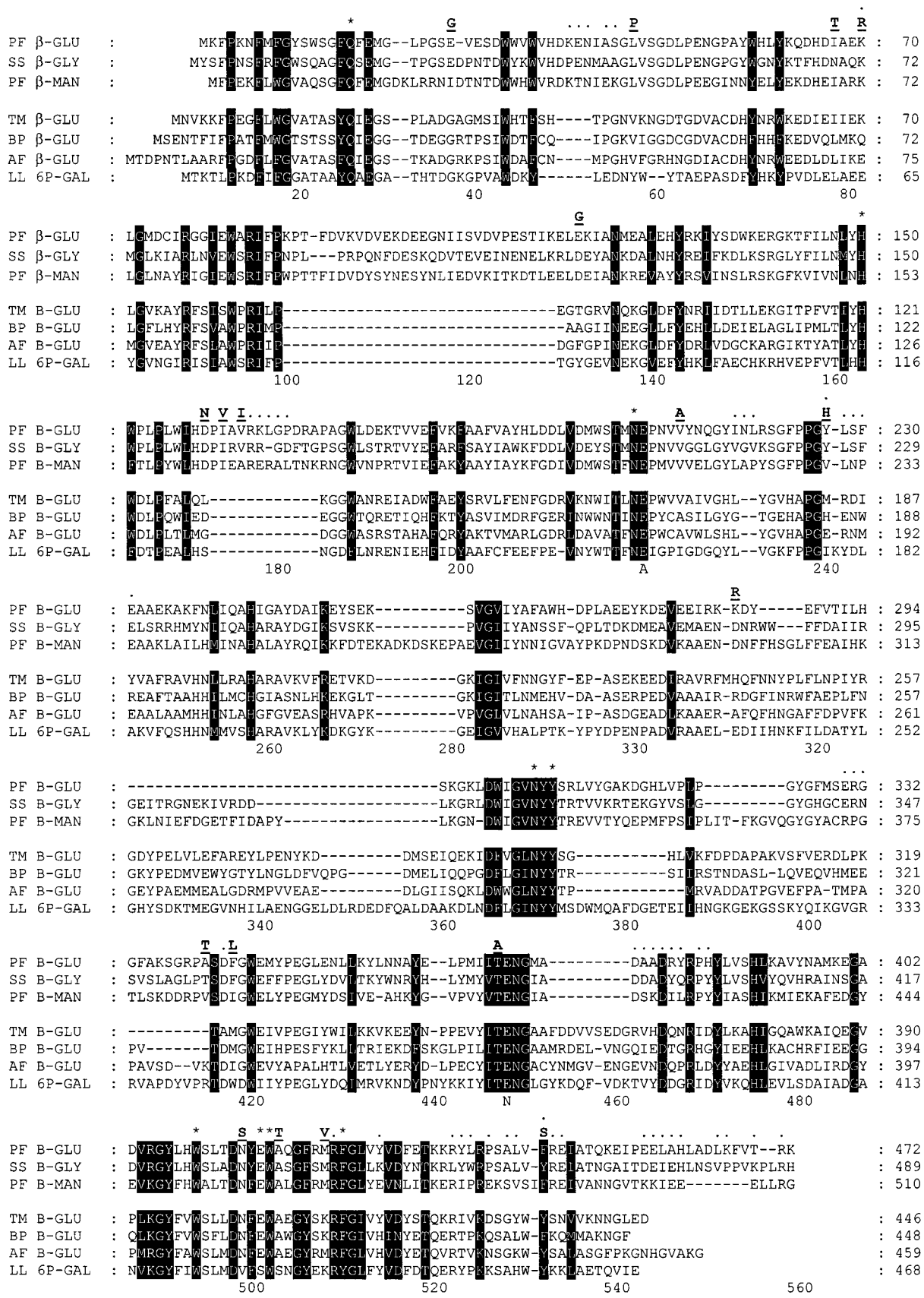

FIGURE 1: Alignment of family 1 glycosylhydrolases. Sequences are obtained from GenBank and include Pf $\beta$-Glu = $\beta$-glucosidase (CelB) from *P. furiosus* (AF013169), Ss $\beta$-Gal = $\beta$-galactosidase (LacS) from *S. solfataricus* (M346g6), Pf $\beta$-man = $\beta$-mannosidase from *P. furiosus* (U60214), Tm $\beta$-Glu = $\beta$-glucosidase from *T. maritima* (X74163), Bp $\beta$-Glu = $\beta$-glucosidase (BglA) from *B. polymyxa* (M60211), Af $\beta$-Glu = $\beta$-glucosidase (Abg) from *A. faecalis* (M1g033), Ll 6P-Gal = 6-phospho-$\beta$-galactosidase (LacG) from *L. lactis* (M28357). The active-site nucleophile and acid−base catalyst are marked with N and A below the sequences, respectively, and other active-site residues are marked with an asterisk. Residues involved in intersubunit interactions are indicated with dots. Identified amino acid substitutions in high-performance mutants are indicated in boldface type and underlined.

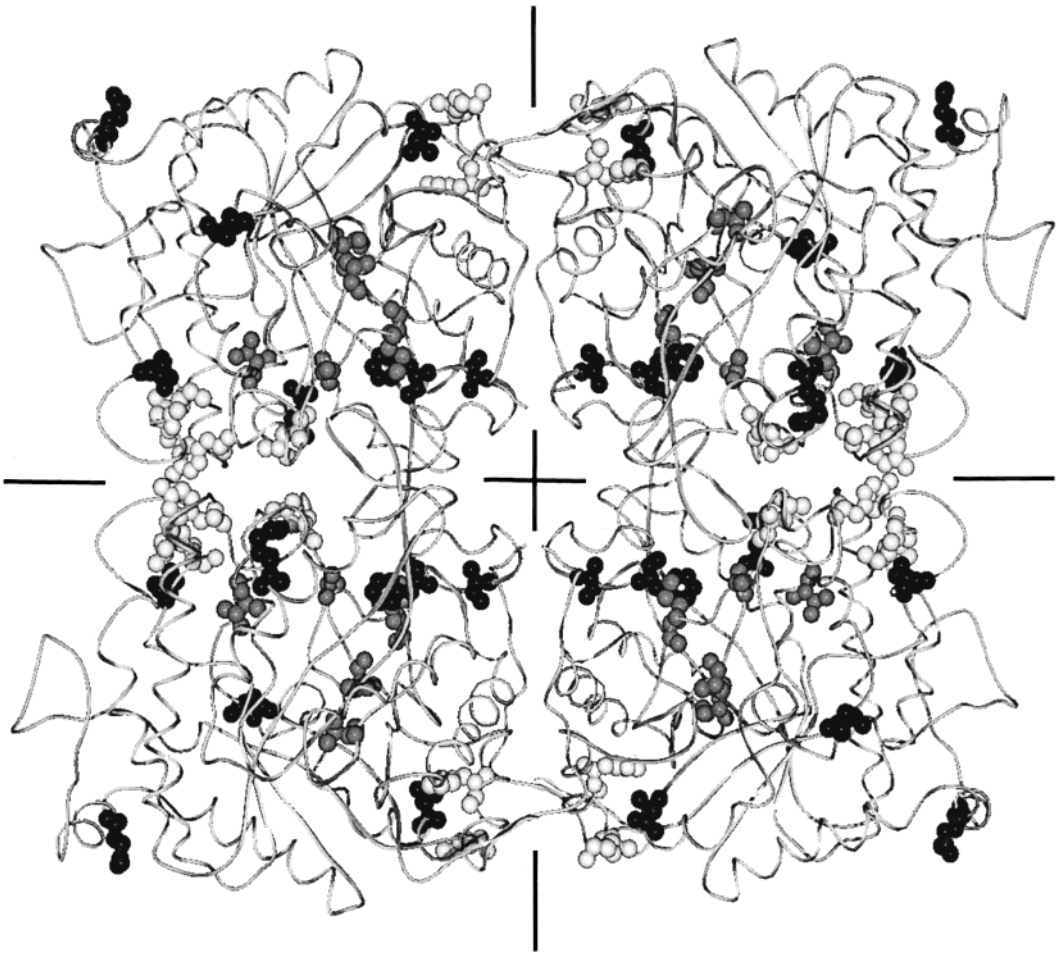

FIGURE 2: Model of the CelB tetramer based on 3.3 Å X-ray diffraction data (*39*, *40*). Subunits are depicted in light-gray ribbon presentation. The amino acids that have been substituted in the high-perfomance CelB mutants are shown in space-filling presentation with class I substitutions in dark gray, class II substitutions in light gray, and class III substitutions in black. The figure has been generated with Swiss PDB viewer (Glaxo Welcome Experimental Research) in combination with the ray tracing program POV-RAY.

tion of this active-site glutamate. Residues at position 424 in homologous enzymes are either methionine or lysine, which both have long, unbranched side chains (Figure 1). In LacG this lysine, together with a serine instead of E417, and a third conservative mutation (a tyrosine at position 426 instead of phenylalanine), serves to stabilize binding of the negatively charged phosphate group on the substrate (*4*, *40*).

Plasmid pLUW843 encodes T371A CelB, with a substitution that results in the removal of the polar side chain of a threonine residue that is located adjacent to the catalytic nucleophile E372. Although this threonine does not seem to interact directly with the glutamate side chain, the fact that this residue and several adjacent residues are completely conserved in all family 1 glycosylhydrolases strongly suggests that interactions in this region are critical for correct catalysis (Figure 1).

Plasmid pLUW846 encodes A419T CelB, which involves a buried alanine at the top of the active-site barrel next to W418 that interacts with the hydroxyl group at the C3 position of the substrate. Because the alanine is buried, the larger threonine side-chain will probably change the side chain packing in this area. Remarkably, the same substitution into threonine or into the similar polar residue serine has also occurred in 6-phospho-$\beta$-galactosidases (Figure 1) (*25*).

Another plasmid that contains only a single base change in the *celB* gene is pLUW844, coding for the amino acid substitution K285R. This mutation is located at the kink in the $\alpha$-helix that creates a tunnel in the side of the $(\alpha\beta)_8$ barrel, which probably forms the substrate entrance to the active site (*12*). K285R is, however, a very conservative mutation and the residue is not conserved at all in homologous enzymes. The model of CelB predicts an ion-pair interaction between K285 and E281, which may still be formed in the mutant K285R CelB.

The fifth substitution in the active-site region, although not as close to the active site itself as the other substitutions, is V211A, which involves a completely buried valine in the same $\alpha$-helix as active-site residues N206 and the acid/base catalyst E207. Residues at this position are always hydrophobic and the mutation will introduce a cavity. This substitution is found in combination with two class II substitutions, V163I and F447S, at the subunit interface in the CelB mutant encoded by pLUW841. The V163I substitution is located in a loop that is only present in the tetrameric family 1 enzymes. The phenylalanine at position 447 is completely buried close to the subunit interface and its substitution to serine will therefore result in a cavity. The aromatic ring at this position in the enzyme seems to be important, since in all family 1 enzymes either a phenylalanine or a tyrosine residue is present.

Two of the above-mentioned active-site substitutions, N415S and V211A, are also present in the enzyme encoded

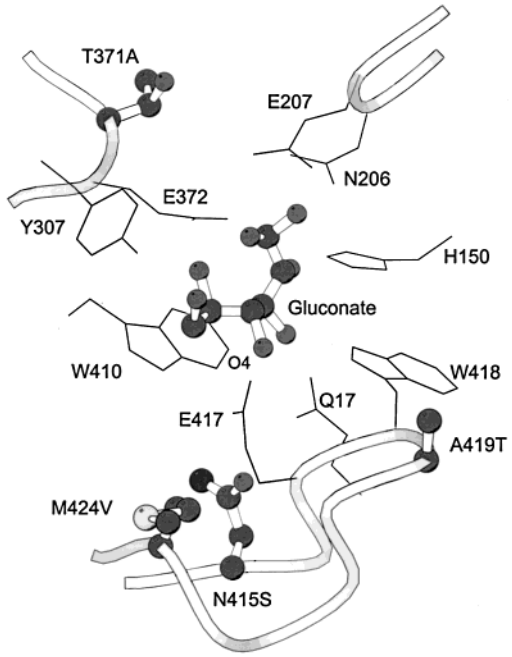


FIGURE 3: Close-up of the active-site of *B. polymyxa* BglA with inhibitor gluconate (*5*). Gluconate is depicted in ball-and-stick representation. Active-site residues are shown in line representation. Corresponding residues that are changed in the high-performance CelB mutants (T371A, M424V, N415S, and A419T) are shown in ball-and-stick representation. Numbering of the residues is according to the homologous CelB residues in order to allow comparison with the text. The figure has been generated with Molscript (*38*).

by plasmid pLUW847 that was selected from a second-generation library. The N415S substitution is derived from the template plasmid in the DNA shuffling procedure; the V211A substitution is introduced independently in this second round of evolution. Two additional mutations are present in pLUW847, resulting in E26G, in which a surface-exposed charge is removed, and Y227H, in which intersubunit interactions are changed. This second-generation CelB variant is significantly more active at room temperature than N415S CelB and exceeds the wild-type CelB activity by more than 3-fold (Table 1).

Two mutants contain multiple substitutions belonging to class II and III. pLUW845 codes for substitution I161V, which is also located in the subunit interface loop that appears to be restricted to tetrameric members of family 1 enzymes. Furthermore, the surface-exposed E119 has been exchanged for a glycine. This may result in the loss of electrostatic interactions and may have significant effects on the local flexibility of the polypeptide because of the large conformational freedom that is introduced with the glycine residue. pLUW840 codes for three substitutions: K70R, L45P, and F344L. This triple mutant is highly destabilized, possibly mainly by the L45P substitution in which the conserved leucine is changed to a proline, that may introduce severe strain into the polypeptide chain.

Plasmid pLUW838 codes for three class III substitutions, viz., I67T, D159N, and A341T. This CelB mutant displays an unchanged temperature optimum curve, is as thermostable as the wild-type enzyme, and shows relatively minor effects on activity (Table 1). These properties indicate that even a highly optimized, hyperthermostable enzyme is able to incorporate changes without losing stability and thermoactivity. None of these residues is completely conserved among close relatives, and moreover, LacS also contains a threonine at position 341 (Figure 1).

*Characterization of High-Performance CelB Variants*. The increase in the rate of $\beta$-glucosidase activity on pNp-Glc at 20 °C that is found in the heat-stable extract of the first-generation mutants differs from 1.1- to 2.6-fold (Table 1). A further increase to more than 3-fold higher activity was obtained in the second-generation mutant. However, $\beta$-galactosidase activity is increased in only four of the mutant CelB enzymes, is unchanged in three other mutants, and has decreased in the remaining three mutant CelB enzymes (Table 1). The largest increase in the ratio of pNp-Glc/pNp-Gal hydrolysis is observed in the mutants containing the active-site-associated mutation N415S (pLUW839 and pLUW847) as well as in the enzyme encoded by pLUW845. This latter mutant CelB is remarkable because its amino acid substitutions are at the enzyme surface (E119G) and on the subunit interface (I161V), indicating that substrate specificity is not solely determined by interactions in the active-site region. Large reductions in both $\beta$-glucosidase and $\beta$-galactosidase activity at 90 °C are found in the mutant CelB mutants, except for the enzyme encoded by plasmid pLUW841 that has increased activity on both substrates, the active-site mutant T371A that has unchanged activity, and, again remarkably, the CelB mutant encoded by pLUW845 that shows increased $\beta$-galactosidase activity, although this was severely reduced at room temperature.

To study whether the low-temperature adaptation of the mutant enzymes affected the activities at other temperatures, their temperature optima were determined. Changes that were detected in the optimum curves could be divided in three categories (Figure 4); (i) flattening of the curve, as is found for mutant N415S (Figure 4a), which shows below 50 °C higher activity than the wild-type CelB, while the reverse was observed above 60 °C; (ii) shifting of the curve to lower temperature values, as observed for mutant M424V (Figure 4b); and (iii) a much earlier inactivation, as found for the mutant encoded by pLUW840 (Figure 4c). All mutants with lower temperature optima for activity also have a lower resistance toward thermal inactivation (Table 1).

*Purification and Thermal Inactivation of Wild-Type and Active-Site Mutant CelB*. To gain more insight in the effects realized by the amino acid changes in the vicinity of the active-site, we decided to purify and characterize mutant CelB enzymes containing a single substitution in this region, namely, N415S, M424V, T371A, and A419T. To obtain an accurate measure of the persistence of catalytic function at high temperature, thermal inactivation of purified wild-type and CelB mutants was followed in time (Table 2). Mutant N415S CelB is as thermostable as the wild-type enzyme, while the other mutants are considerably destabilized; compared to all other family 1 glycosylhydrolases they are, however, still extremely thermostable enzymes because they all retain a considerable amount of activity after incubation at 106 °C.

*Kinetic Characterization of Wild-Type CelB at 20 and 90 °C*. The hydrolysis of pNp-GlC by wild-type CelB revealed an apparent inhibition in a hyperbolic Michaelis−Menten plot, starting at substrate concentrations above 1 mM at 20 °C (Figure 5) and above 2−4 mM pNp-Glc at 90 °C (not shown). A similar phenomenon was observed during cello-

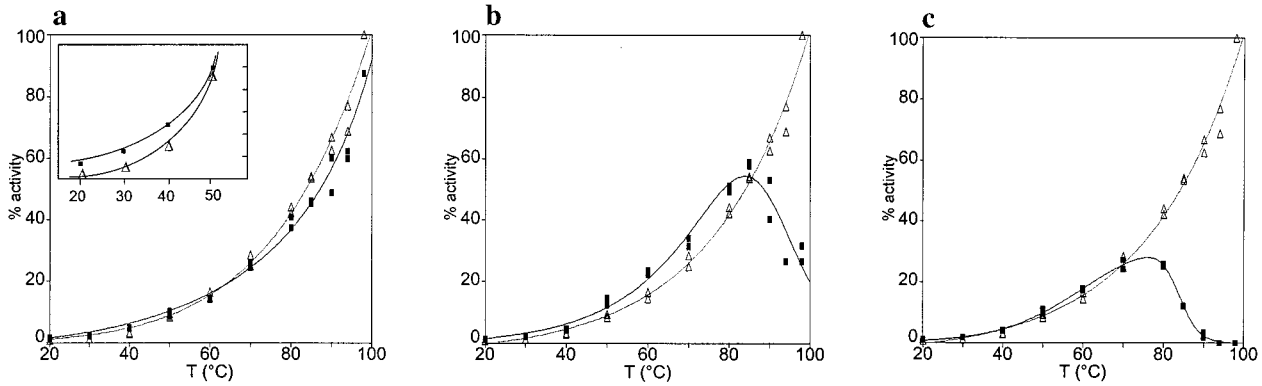


FIGURE 4: Optimum temperature curve for wild-type CelB (△ in all panels) compared to (a) mutant CelB N415S (■), (b) mutant CelB M424V (■), and (c) mutant CelB K70R/L45P/F344L (■). The inset in panel a zooms in on the increased activity of N415S CelB below 50 °C.

Table 2: Kinetic Parameters of Wild-Type and Mutant CelB Enzymes at 20 °C on PNp-Glc, PNp-Gal, and $\beta$(1,4)-Linked Disaccharides Cellobiose and Lactose[a]

| | pNp-Glc | | | cellobiose | | | pNp-Gal | | | lactose | | | thermostability |
|---|---|---|---|---|---|---|---|---|---|---|---|---|---|
| CelB variant | $k_{cat}$ ($s^{-1}$) | $K_m$ (mM) | cat. eff[a] ($mM^{-1}$ $s^{-1}$) | $k_{cat}$ ($s^{-1}$) | $K_m$ (mM) | cat. eff ($mM^{-1}$ $s^{-1}$) | $k_{cat}$ ($s^{-1}$) | $K_m$ (mM) | cat. eff ($mM^{-1}$ $s^{-1}$) | $k_{cat}$ ($s^{-1}$) | $K_m$ (mM) | cat. eff ($mM^{-1}$ $s^{-1}$) | $t_{1/2}$ at 106 °C (h) |
| wild-type | 13 | 0.53 | 25 | 16 | 23 | 0.69 | 9.1 | 0.70 | 13 | 13 | 52 | 0.25 | 3.3 |
| N415S | 47 | 1.1 | 43 | 20 | 20 | 1.0 | 4.2 | 1.2 | 3.5 | 21 | 95 | 0.22 | 3.2 |
| M424V | 40 | 0.92 | 43 | 18 | 16 | 1.1 | 12 | 3.4 | 3.4 | 21 | 97 | 0.22 | 1.1 |
| T371A | 26 | 0.57 | 45 | 15 | 11 | 1.4 | 11 | 1.3 | 8.2 | 17 | 52 | 0.33 | 0.65 |
| A419T | 40 | 1.3 | 31 | 19 | 25 | 0.75 | 14 | 4.5 | 3.1 | 15 | 83 | 0.18 | 0.82 |

[a] In the last column the half-life of thermal inactivation at 106 °C Is listed. [b] Catalytic efficiency = $k_{cat}/K_m$.

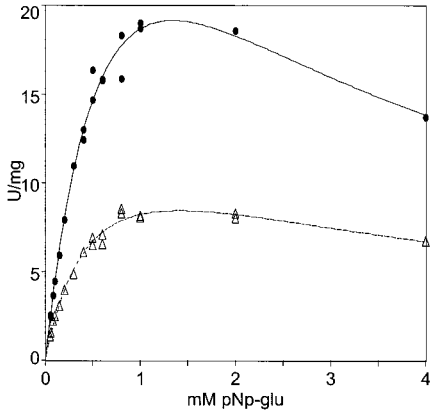


FIGURE 5: Comparison of rate of pNp-Glc hydrolysis by wild-type (△) and mutant CelB N415S (●) as a function of substrate concentration at 20 °C.

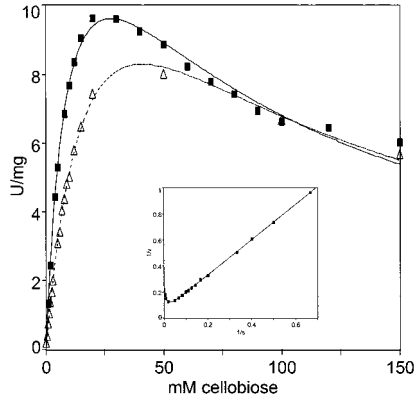


FIGURE 6: Comparison of the rate of cellobiose hydrolysis by wild-type (△) and mutant T371A CelB (■) as a function of substrate concentration at 20 °C. Inset: Lineweaver−Burk plot for wild-type CelB.

biose hydrolysis (Figure 6). Plotting the data according to a Lineweaver−Burk equation resulted in a curve typically found when substrate inhibition occurs (inset in Figure 6). This process has not been reported in the previous kinetic characterization of CelB, presumably because employed maximum substrate concentrations did not exceed 1.5 mM pNp-Glc at 90 °C (*15*). Apparent substrate inhibition was, however, also observed with the $\beta$-glucosidase from *T. maritima* (*6*). Fitting of the data according to Michaelis−Menten kinetics, corrected for substrate inhibition, resulted in a $k_{cat}$ of 13 $s^{-1}$ and a $K_m$ of 0.53 mM for pNp-glucose at 20 °C (Table 2). The enzyme is 2-fold less efficient on pNp-Gal than on pNp-Glc, due to a lower hydrolysis rate and a lower affinity for the galactosyl substrate. On cellobiose and lactose, similar $k_{cat}$ values are found, but affinity for the $\beta$(1,4)-linked disaccharides is relatively low. $k_{cat}$-values for the aryl glycosides at 90 °C are 1.5- and 4-fold higher than reported earlier for the enzyme purified from *E. coli* by Voorhorst et al. and by Bauer and Kelly, respectively (*9*, *15*). This difference may be related to the observed substrate inhibition or may reflect the variability between independent enzyme preparations that have been purified by different methods. Calculated $K_m$ values at 90 °C are more or less similar to those already reported. Interestingly, while $K_m$ values of wild-type CelB for pNp-Glc and cellobiose at 90 °C *decrease* compared to those at 20 °C, these values *increase* for pNp-Gal and lactose. Substrate affinity is, apparently, highly influenced by the operation temperature. It should be noted that, although $k_{cat}$ values for pNp-Gal and lactose are considerably higher than for pNp-Glc and cellobiose, the enzyme shows, based on catalytic efficiency, a higher $\beta$-glucosidase than $\beta$-galactosidase activity.

Table 3: Kinetic Parameters of Wild-Type CelB and Mutant N415S at 90 °C on PNp-Glc, PNp-Gal, and $\beta$(1,4)-Linked Disaccharides Cellobiose and Lactose

| | pNp-Glc | | | cellobiose | | | pNp-Gal | | | lactose | | |
|---|---|---|---|---|---|---|---|---|---|---|---|---|
| CelB variant | $k_{cat}$ ($s^{-1}$) | $K_m$ (mM) | cat eff[a] ($mM^{-1}$ $s^{-1}$) | $k_{cat}$ ($s^{-1}$) | $K_m$ (mM) | cat. eff ($mM^{-1}$ $s^{-1}$) | $k_{cat}$ ($s^{-1}$) | $K_m$ (mM) | cat. eff ($mM^{-1}$ $s^{-1}$) | $k_{cat}$ ($s^{-1}$) | $K_m$ (mM) | cat. eff ($mM^{-1}$ $s^{-1}$) |
| wild type | 1600 | 0.42 | 3900 | 670 | 14 | 48 | 2400 | 5.0 | 480 | 1300 | 120 | 11 |
| N415S | 1400 | 1.4 | 1000 | 240 | 38 | 6.4 | 1000 | 8.5 | 120 | 530 | 220 | 2.4 |

[a] Catalytic efficiency = $k_{cat}/K_m$.

*Transglycosylation*. Transglycosylation is common among family 1 glycosylhydrolases. It has been described before for *P. furiosus* CelB and *A. faecalis* Abg in the case of pNp-xylose and pNp-arabinose substrates and for CelB as well with cellobiose and lactose (*15*, *26*−*28*). Cellotriose formation from cellobiose has been reported for BglA from *B. polymyxa* and for the $\beta$-glucosidase from *T. maritima* (*29*, *6*). Analysis of reaction products of CelB incubated with 150 mM cellobiose by HPLC revealed, apart from glucose and cellobiose, the presence of an additional product with the same retention time as cellotriose, strongly suggesting that transglycosylation is indeed occurring. Kinetic characterization of this process was not possible because its effect on product formation was completely masked by the large observed substrate inhibition (see above).

*Kinetic Characterization of Active-Site Mutant CelB Enzymes at 20 °C*. The catalytic efficiencies of mutated CelB on pNp-Glc and cellobiose are increased up to 2-fold in comparison with wild-type CelB (Table 2). This has either been achieved by large increases in $k_{cat}$ values, as in the case of mutant N415S CelB on pNp-Glc (Figure 5a), or by a decrease in $K_m$ values, as observed for T371A CelB on cellobiose (Figure 5b). The increase in efficiency of pNp-Glc hydrolysis is at the expense of catalytic efficiency on pNp-Gal. However, a similar effect is not observed on $\beta$(1,4)-linked disaccharides; moreover, a significant increase in efficiency is reported for T371A CelB on lactose. Evidently, the effect of the leaving group (either pNp or glucose for the aryl glycosides and the disaccharides, respectively) on catalytic efficiency is not comparable for glucosyl and galactosyl substrates. This is most clearly illustrated for mutant N415S CelB, for which a large reduction in maximum activity on pNp-galactose is found, which is now more than 10-fold lower than maximum activity on pNp-glucose. In contrast, cellobiose is hydrolyzed with the same maximum velocity as lactose. The mutant enzymes show, in general, a higher substrate inhibition than the wild-type CelB, because the substrate concentration at which the activity is reduced to $^1/_2$ $V_{max}$ is lower for all the mutants than for the wild-type CelB (results not shown).

*Kinetic Characterization of Active-Site Mutant CelB N415S at 90 °C*. Because N415S CelB is as thermoactive and thermostable as the wild-type CelB, we decided to analyze its kinetic parameters at 90 °C in order to see the relation between these characteristics at low and high temperatures (Table 3). The maximum activity of mutant N415S CelB at 90 °C was lower than for the wild-type enzyme for pNp-Glc and especially pNp-Gal. Because also $K_m$ values increase, N415S CelB is less efficient than wild-type CelB on pNp-Glc and pNp-Gal. The same is found for the disaccharides. Higher performance on pNp-Glc at room temperature is therefore not only at the expense of galactosidase activity at room temperature but also at the expense of high-temperature catalysis. Because of the apparent unchanged temperature optimum and thermostability of this mutant, this effect is not caused by an overall destabilization of the enzyme but must be a direct result of the effects of the single mutation on substrate binding and turnover rates.

## CONCLUSIONS

Screening of a random CelB library resulted in the selection of CelB variants with significantly higher activity on pNp-Glc at room temperature than the wild-type enzyme. Amino acid substitutions were located in the active-site region (class I), at or close to subunit interfaces (class II), or either at the protein surface or buried in the subunit interior (class III). All mutants containing subunit interface substitutions were less thermostable and had lower temperature optima than the wild-type CelB, suggesting that subunit interfaces play an important role in thermoadaptation. Hyperthermostable enzymes are most probably highly optimized with respect to packing efficiency (*30*, *31*). However, a recent database survey showed that proteins from mesophiles and thermophiles essentially do not differ in packing (*32*). The present study indicates that CelB is able to accommodate amino acids in its interior with larger or smaller side chains and different properties, without affecting its thermostability or temperature optimum for catalysis. Interestingly, none of the mutants displayed intact thermostability and increased activity at both low and high temperatures. This observation might indicate that CelB is highly optimized regarding both stability and flexibility and that severe restrictions exist on the simultaneous optimization of these intimately related parameters.

Remarkably, substrate specificity of CelB seems to be a characteristic that is determined by the enzyme as a whole, since changes in the ratio on pNp-Glc and pNp-Gal are not restricted to substitutions in the active-site region. However, the most drastic effect on the pNp-Glc/pNp-Gal ratio (a 7.5-fold increase) is caused by the disruption of interactions between asparagine at position 415 and two active-site residues that directly contact the hydroxyl group on the substrate at the C4 position. This is exactly the (only) position at which glucose and galactose differ in orientation of this hydroxyl group. The loss of hydrogen bonds between the substituted asparagine and active-site residues Q17 and E417 may influence the position and the flexibility of these side chains, thereby changing their interactions with the substrate and the ratio between binding and turnover on substrates with either glucose or galactose moieties at this position. This is indeed found for mutant N415S on aryl glycosides and, to a lesser extent, on $\beta$(1,4)-linked disaccharides. In fact, a key role in determining glucose/galactose specificity for residues interacting with the active-site Q17 and E417 was proposed

recently on the basis of the interactions between the inhibitor gluconate and active-site residues of *B. polymyxa* BglA (*5*). Further indications that slight changes in conformational freedom of active-site residues may have large effects on catalysis and substrate recognition is provided by the large and opposing effect of operational temperature on affinities for different substrates. While wild-type CelB has 8-fold higher efficiency on pNp-glucose than on pNp-galactose at 90 °C, this ratio is reduced to 2-fold at 20 °C. Until recently it was assumed, based on lactate dehydrogenase from *Thermotoga maritima* and *T. neapolitana* xylose isomerase, that an increased temperature causes the decrease of one enzyme's affinity for its substrate (*33*−*35*). However, the results presented here indicate that this assumption does not hold. Also, for glutamate dehydrogenase from *P. furiosus* and *T. maritima* we have reported different changes in substrate affinity with increasing temperature, depending on the substrate (*36*, *37*).

Our results show that the quality of the random CelB library is good and that the sensitivity of the screening procedure is sufficient to isolate mutants with only 10% increase in activity. Mutants displaying evolved properties, like N415S CelB with 2-fold increased catalytic efficiency on pNp-Glc but unchanged stability, and mutant T371A CelB with 2-fold higher affinity for cellobiose, could be interesting candidates for industrial or diagnostic applications.

In conclusion, this random screening approach with a hyperthermostable enzyme resulted in the identification of residues that are critical in determining thermostability, low-temperature activity, and substrate recognition. It was shown that low-temperature activity can be engineered into a hyperthermostable enzyme without affecting its extreme stability. Not only is directed evolution a powerful approach to introduce a desired property into an industrially relevant biocatalyst, but as we have shown here, it may facilitate our understanding of the mechanisms determining enzyme catalysis, stability, and substrate recognition at physiological or extreme conditions.

## ACKNOWLEDGMENT

We are very grateful to Servé Kengen (Laboratory of Microbiology, Wageningen University) for helpful discussion, to Ans Geerling and Ineke Heikamp-de Jong (Laboratory of Microbiology, Wageningen University) for technical assistance, and to Leo de Graaff (Molecular Genetics of Industrial Microorganisms, Wageningen University) for kindly providing access to a microtiter plate reader.

## REFERENCES

1. Davies, G., and Henrissat, B. (1995) *Structure 3*, 853−9.
2. Henrissat, B., and Davies, G. (1997) *Curr. Opin. Struct. Biol. 7*, 637−644.
3. Wiesmann, C., Beste, G., Hengstenberg, W., and Schulz, G. E. (1995) *Structure 3*, 961−8.
4. Wiesmann, C., Hengstenberg, W., and Schulz, G. E. (1997) *J. Mol. Biol. 269*, 851−860.
5. Sanz-Aparicio, J., Hermoso, J. A., Martinez-Ripoll, M., Lequerica, J. L., and Polaina, J. (1998) *J. Mol. Biol. 275*, 491−502.
6. Gabelsberger, J., Liebl, W., and Schleifer, K.-H. (1993) *Appl. Microb. Biotechnol. 40*, 44−52.
7. Cubellis, M. V., Rozzo, C., Montecucchi, P., and Rossi, M. (1990) *Gene 94*, 89−94.
8. Pisani, F. M., Rella, R., Raia, C. A., Rozzo, C., Nucci, R., Gambacorta, A., De Rosa, M., and Rossi, M. (1990) *Eur. J. Biochem. 187*, 321−8.
9. Voorhorst, W. G., Eggen, R. I., Luesink, E. J., and de Vos, W. M. (1995) *J. Bacteriol. 177*, 7105−11.
10. Kengen, S. W., Luesink, E. J., Stams, A. J., and Zehnder, A. J. (1993) *Eur. J. Biochem. 213*, 305−12.
11. Bauer, M. W., Bylina, E. J., Swanson, R. V., and Kelly, R. M. (1996) *J. Biol. Chem. 271*, 23749−55.
12. Aguilar, C. F., Sanderson, I., Moracci, M., Ciaramella, M., Nucci, R., Rossi, M., and Pearl, L. H. (1997) *J. Mol. Biol. 271*, 789−802.
13. Chi, Y.-I., Martinez-Cruz, L. A., Jancarik, J., Swanson, R. V., Robertson, D. E., and Kim, S.-H. (1999) *FEBS Lett. 445*, 375−383.
14. Driskill, L. E., Bauer, M. W., and Kelly, R. M. (1999) *Appl. Environ. Microbiol. 65*, 893−7.
15. Bauer, M. W., and Kelly, R. M. (1998) *Biochemistry 37*, 17170−8.
16. Stemmer, W. P. (1994) *Proc. Natl. Acad. Sci. U.S.A. 91*, 10747−51.
17. Kuchner, O., and Arnold, F. H. (1997) *Trends Biotechnol. 15*, 523−530.
18. Arnold, F. H. (1998) *Acc. Chem. Res. 31*, 125−131.
19. Lorimer, I. A., and Pastan, I. (1995) *Nucleic Acids Res. 23*, 3067−8.
20. Rosenberg, A. H., Lade, B. N., Chui, D. S., Lin, S. W., Dunn, J. J., and Studier, F. W. (1987) *Gene 56*, 125−35.
21. Studier, F. W., Rosenberg, A. H., Dunn, J. J., and Dubendorff, J. W. (1990) *Methods Enzymol. 185*, 60−89.
22. Yanisch-Perron, C., Vieira, J., and Messing, J. (1985) *Gene 33*, 103−19.
23. Bradford, M. M. (1976) *Anal. Biochem. 72*, 248−54.
24. Gill, S. C., and von Hippel, P. H. (1989) *Anal. Biochem. 182*, 319−26.
25. Witt, E., Frank, R., and Hengstenberg, W. (1993) *Protein Eng. 6*, 913−20.
26. Kempton, J. B., and Withers, S. G. (1992) *Biochemistry 31*, 9961−9.
27. Fischer, L., Bromann, R., Kengen, S. W. M., Devos, W. M., and Wagner, F. (1996) *Bio/Technology 14*, 88−91.
28. Boon, M. A., Van der Oost, J., De Vos, W. M., Janssen, A. E. M., and Van't Riet, K. (1999) *Appl. Biochem. Biotechnol. 75*, 269−278.
29. Painbeni, E., Valles, S., Polaina, J., and Flors, A. (1992) *J. Bacteriol. 174*, 3087−91.
30. Jaenicke, R., and Bohm, G. (1998) *Curr. Opin. Struct. Biol. 8*, 738−748.
31. Scandurra, R., Consalvi, V., Chiaraluce, R., Politi, L., and Engel, P. C. (1998) *Biochimie 80*, 933−941.
32. Karshikoff, A, L. R. (1998) *Protein Eng. 11*, 867−72.
33. Hecht, K., Wrba, A., and Jaenicke, R. (1989) *Eur. J. Biochem. 183*, 69−74.
34. Vieille, C., Hess, J. M., Kelly, R. M., and Zeikus, J. G. (1995) *Appl. Environ. Microbiol. 61*, 1867−75.
35. Vieille, C., and Zeikus, J. G. (1996) *Trends Biotechnol. 14*, 183−190.
36. Lebbink, J. H. G., Eggen, R. I. L., Geerling, A. C. M., Consalvi, V., Chiaraluce, R., Scandurra, R., and de Vos, W. M. (1995) *Protein Eng. 8*, 1287−94.
37. Lebbink, J. H. G., Knapp, S., van der Oost, J., Rice, D., Ladenstein, R., and de Vos, W. M. (1998) *J. Mol. Biol. 280*, 287−96.
38. Kraulis, P. J. (1991) *J. Appl. Crystallogr. 24*, 946−950.
39. Kopp, J. (1998) Ph.D. Thesis, Universität Freiburg, Germany.
40. Kaper, T., Lebbink, J. H. G., Pouwels, J., Kopp, J., Schulz, G. E., van der Oost, J., and de Vos, W. M. (2000) *Biochemistry* (in press).

BI991483Q